MORPHOLOGY, PATHOLOGY, PHYSIOLOGY

DOI 10.35630/2023/13/3.308

Received 14 May 2023;
Accepted 20 June 2023,
Published 23 June 2023

HISTOMORPHOMETRIC ASSESSMENT OF ARCHITECTONICS AND VASCULARIZATION IN MAXILLARY ALVEOLAR PROCESS BONE TISSUE

***Dmitry Domenyuk*[1] ✉, *Olga Sumkina*[1],**
***Natalya Mikutskaya*[1], *Taisiya Kochkonyan*[2],**
***Andrey Markovsky*[1], *Dmitry Matsukatov*[1],**
***Yuriy Harutyunyan*[1], *Oleg Ivanyuta*[1],**
***Stanislav Domenyuk*[3]**

[1] *Stavropol State Medical University, Stavropol;*
[2] *Kuban State Medical University, Krasnodar;*
[3] *North Caucasus Federal University, Stavropol, Russia*

✉ ***domenyukda@mail.ru***

download article (pdf)

ABSTRACT

The expansion of the most relevant priority fields in fundamental and applied medicine, along with the progress in modern dentistry and reconstructive maxillofacial surgery, requires in-depth understanding of the morphological and functional status of the maxillary alveolar process bone tissue and knowledge of the mandibular alveolar part, thus allowing selecting a reasonable treatment tactics for maxillofacial pathologies.

Qualitative features of maxillary alveolar process microarchitectonics, angioarchitectonics, as well as the periodontal ligament arrangement at various levels of the teeth roots, histological and morphometric studies of bone tissue in the frontal and distal sections, as well as the maxillary segments of the maxillary medial incisors and the first molars were studied in 5 certified male cadavers with preserved dentition. The histological findings show, that the microarchitectonics of the maxillary alveolar process features a lamellar bone consists of plates that are adjacent tightly to each other.

The bone plates orientation in the frontal section is longitudinal, while in the distal part it is along concentric circles located around the Haversian canals. The angioarchitectonics of the maxillary alveolar process features tubular structures, which run mainly perpendicular to the bone surface, with numerous anastomoses. As the morphometric analysis of the maxillary alveolar process vascular system shows, in the frontal section the number of vessels per 1 mm^2 is 22.41± 1.76 - 22.87± 2.08; in the distal section – 23.94± 1.88 - 25.02±2.69 ($p \leq 0.01$); the average diameter of vessels in the frontal section is 25.34±2.45 microns – 26.06 ±3.17 microns, in the distal section – 25.72±2.31 microns – 26.14± 2.93 microns ($p \leq 0.05$); the average wall thickness in the frontal section is 1.43± 0.09 microns - 1.48± 0.12 microns, in the distal section – 1.50± 0.11 microns – 1.54± 0.14 microns ($p \leq 0.01$).

The vestibular surface of the maxillary medial incisors at the level of the root gingival part, as well as the oral surface at the root apical level have been found to be zones of *periodontal ligament compression*, while the oral surface at the root gingival level and the vestibular surface at the root apical level – zones of *the periodontal ligament stretching*. At the root gingival level of the first maxillary molars, the medial and vestibular surfaces are zones of *the periodontal ligament compression*, whereas the oral and the distal

surfaces stand as the zones of *the periodontal ligament stretching*.

As a quantitative assessment showed, the structural elements of the medial incisors periodontal ligament, and the first maxillary molars had loose connective tissue – taken by its specific area – prevailing in the periodontal ligament compression zone; the specific area of dense connective tissue, though, was found to be prevailing at the periodontal ligament stretching zone under chewing stress. The data obtained through a quantitative analysis of the periodontal ligament microvascular bed of the medial incisors, and the first maxillary molars, reveal that the area with blood vessels in the *compression* zones by far exceeds the area of blood vessels in the *stretching* zones. It appears rather reasonable that in case of a biomechanical stress experienced by the incisor-maxillary and molar-maxillary segments of the upper jaw, the periodontal ligament morphology will change throughout the root, depending on the *compression* and *stretching* zone localization.

Keywords: morphology, bone preparation histological examination, periodontal ligament, maxillary architectonics, morphometric analysis of vascular bed, bone tissue, biomechanics, masticatory stress.

INTRODUCTION

Clinical anatomy, taken as a set of applied areas within modern anatomy, focuses on studying the structure and the topography of organs and areas, both in norm and in case of pathology, thus serving various fields of clinical medicine [1-4].

One of the main areas in clinical anatomy is surgical anatomy focusing on the specific features pertaining to the structure and topography in normal and in pathological conditions. This is of applied value in surgery where there is a need to have sufficient grounds for surgical interventions. Other significant areas belonging to clinical anatomy include X-ray and computed tomography anatomy, which displays the structure and the topography of various organs and areas in images obtained through appropriate intra vitam methods involving X-ray radiation, this being of practical value in terms of expanding knowledge about individual anatomical variability [5-11].

Clinical morphology of the oral cavity, as a section of clinical anatomy that systematizes data regarding the anatomy and topography of the oral cavity organs thus aiming to assist dentistry, contributes to the understanding of the etiological, pathogenetic and specific features of many pathological processes underway in the maxillofacial area [12-19].

The wide introduction of intra vitam imaging (radiography, cone-beam computed tomography, magnetic resonance imaging, ultrasound scanning) that modern clinical dentistry is facing currently, requires a profound understanding of topographic anatomy, while the methods of intra vitam imaging themselves allow early diagnosing of diseases affecting hard tissues of teeth, periodontal, temporomandibular joints, oral mucosa, as well as bone tissues of the facial and cerebral parts of the skull [20-27].

Intra vitam imaging methods, if employed in clinical and anatomical studies, help study the following features: anatomical variability of different organs and areas; changes affecting the topography of organs in case of pathological conditions; changes in the topography of organs following surgical interventions; anatomical explanation for newer surgical approaches and techniques; computer modeling [28-32].

Examining individual, as well as age-, race- and sex-related differences from the human anatomical variability standpoint will allow not only identifying a much wider range of individual anatomical specifics, yet will also help design full scopes of anatomical differences, at the same time pointing at extreme and in-between patterns [33-39].

Intra vitam imaging methods used when examining healthy patients allow not only excluding possible pathological conditions, but also obtaining a large array of anatomical data for shaping morphometric understanding of organs and specific parts, as well as establishing mathematically viable anatomical and functional patterns. Such methods of visualization appear reasonable when developing and explain, from the anatomical point of view, new types of surgical interventions, specifically ensuring surgical access. This said, computed tomography makes it possible to customize the organ projection on the skin and to identify the depth of the required location depending on the body constitution features [40-43].

Bone is a mineralized, vascularized and innervated dense fibrous connective tissue with a certain arrangement of specialized cellular elements, a fibrous base and an extracellular interstitial space, featuring a complex multilevel system of interconnected channels. Bone tissue is a living dynamic structure that is involved in the homeostasis of calcium, phosphorus, carbonate, and other elements, as well as in the acid-base balance regulation. It is in close contact with the hematopoietic system (red bone marrow), where the two share a common pool of progenitor cells and local regulatory factors. The mineral matrix of skeletal bones can bind certain toxins and metal ions, thus minimizing the toxic effects that can affect cells of other organs and tissues [44-48].

Bone tissue serves as a reservoir for many growth factors and cytokines; some of them get synthesized by

the bone cells themselves, to be further secreted into the blood and get involved in metabolic regulation [49-50].

The structural arrangement of bone tissue features woven bone and lamellar bone tissues. The remains of hard fibrous bone tissue that develop through embryogenesis can be observed in adults' dental alveoli, at the cranial sutures, in the inner ear bone labyrinth and near the attachment spots of tendons and ligaments, while in all these places such tissue comes alternating with mature (lamellar) bone tissue. Histologically, hard fibrous bone tissue appears as bundles of coarse collagen fibers arranged randomly into a simple and primitive matrix, whose surface has bone cells of osteoblasts scattered on it. Lamellar bone is a mature bone tissue developing from bone plates (osteones). The bone plate is a multilayer structure, each layer being 4-12 microns of thickness. Osteoblasts, which are involved in consistent formation of mature bone tissue layers, and which appear as osteocytes, are part of the matrix (osteoid) formed by them, staying in lacunae inside its layers or between them. Collagen fibers of one layer are located either at a certain angle towards the fibers of the adjacent layers, or run perpendicular, thus ensuring the strength of lamellar bone tissue. Lamellar bone tissue makes up the compact, or cortical, bone, as well as the spongy cancellous or trabecular bone substance that can be seen in all flat and tubular bones [51].

The physiological properties of bone tissue are subject to change depending on age, nutrition, muscular activity, the nervous and endocrine status, and pathologies affecting internal organs. Bone tissue is capable of adjusting itself to external influences, which caused a change in the internal structure and external shape of the bone. Such architectonics is in charge of the mechanical properties of bone tissue, its resistance to deformation, while the variability of parameters depends on the ratio of the compact and spongy bone tissue, on the location, as well as on individual human factors [52-55].

The basis for the regulation of bone tissue restructuring is continuous modeling and remodeling mechanisms. Modeling is behind the microstructure of the bone during its growth or recovery after an injury, and this process depends on a number of metabolic and mechanical factors, and it involves the coordination of resorption and osteogenesis going on simultaneously in different parts of the tissue. Remodeling implies resorption of local areas and filling of the defects with newly developed bone tissue. Remodeling allows changing the bone volume, shape and density, adjusting in the best way possible to the current loads, while correcting and updating the tissue microarchitectonics [56-58].

The periodontal ligament that holds the tooth root in the bone alveolus is a dense fibrous connective tissue localized in the periodontal space. The main functions of the periodontal ligament are supporting (retaining and cushioning), trophic, homeostatic, reparative, immune protection, and involvement in teething, as well as proprioceptive sensitivity. The high proliferative and functional activity that can be observed in periodontal ligament cells, in collagen renewal mechanisms, and in cement reparation and remodeling of the alveolar bone, offers a significant potential for self-healing under conditions like growth, chewing an undergoing treatment [59].

The periodontium blood and lymphatic vessels are connected – by numerous anastomoses – with the vascular system of the maxillary alveolar process bone tissue, which means that assessing the alveolar bone status is of value in terms of choosing a treatment method for many maxillofacial pathologies [60-62]. A comprehensive assessment of the maxillary alveolar process microarchitectonics and angioarchitectonics (the dentition preserved), while relying on biopsy histomorphometric studies, will allow assessing the structure parameters and qualitative features of intact bone tissue, as well as identifying the balance of the mechanisms behind resorption and bone development, at the cellular and tissue level.

Aim: to study the qualitative features pertaining to the microarchitectonics and angioarchitectonics of the maxillary alveolar process, in case of intact dentition, relying on histomorphometric studies.

MATERIALS AND METHODS

The material for the study was obtained through a sectional examination of 5 certified male bodies with intact dentition at the Thanatology department of the Forensic Examination Bureau. The age of the bodies was within the II adulthood period (36 – 60). The histological and morphometric studies of the bone tissue preparations were done at the Consulting Clinical Pathology Bureau. Inclusion criteria: no traumatic injuries of bone preparations; no signs of pathological changes or signs of diseases (connective tissue diseases, endocrine pathologies; significant signs of chronic exogenous intoxication).

For bone tissue histological examination and for a morphometric analysis of the maxillary alveolar process vascular system, bone blocks were used (5×5 mm in the projection of the medial incisors and the first molars on both sides) (Fig. 1,2).

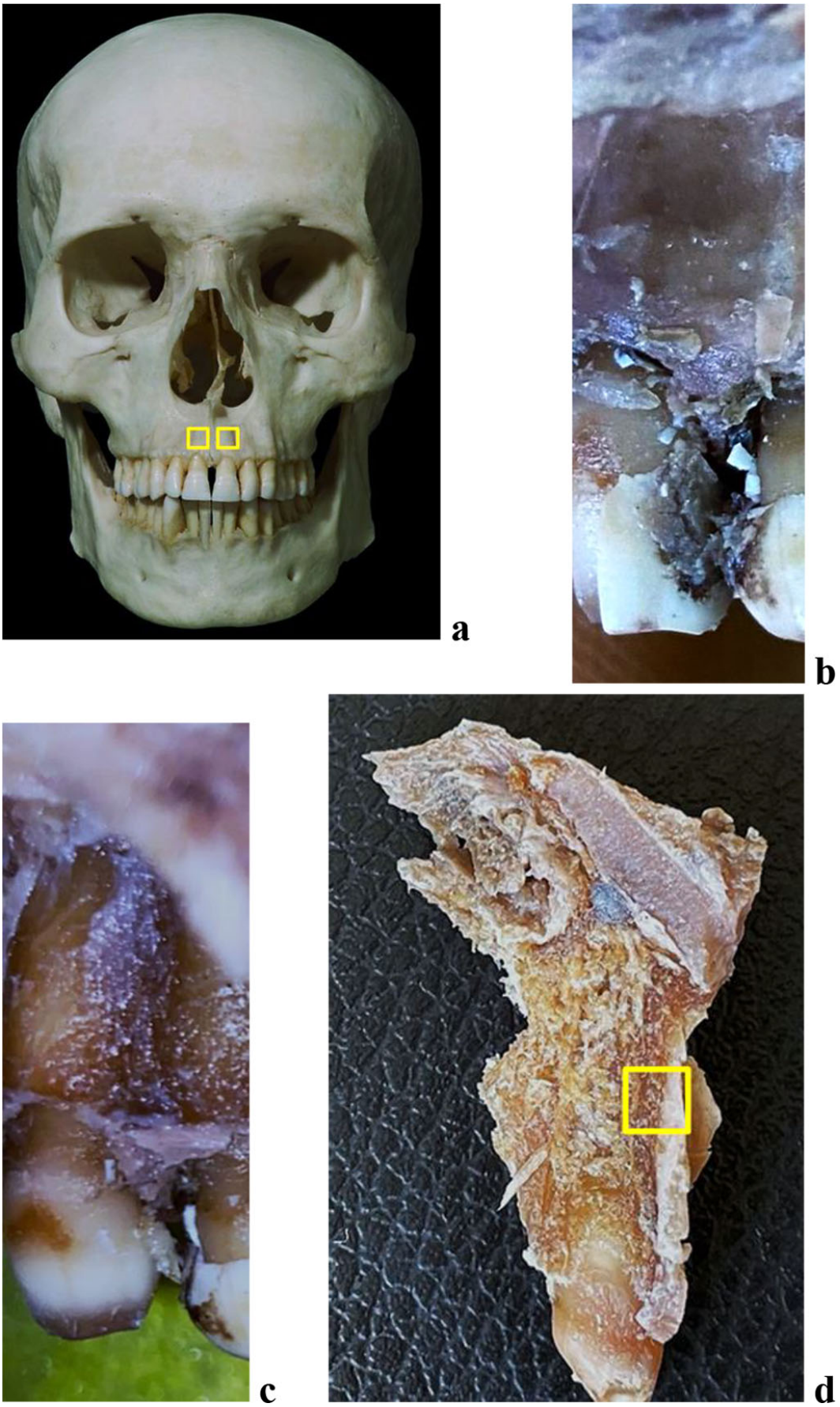

Figure 1. Bone biopsy specimen from the frontal alveolar process of the maxilla with preserved dentition: a – areas for taking bone preparations on the skull; anatomical preparation before (b) and after (c) separation of the muco-periosteal flap in the area of 21 teeth; d – area for taking a bone preparation on the maxillary medial incisor segment of the maxilla (21 teeth).

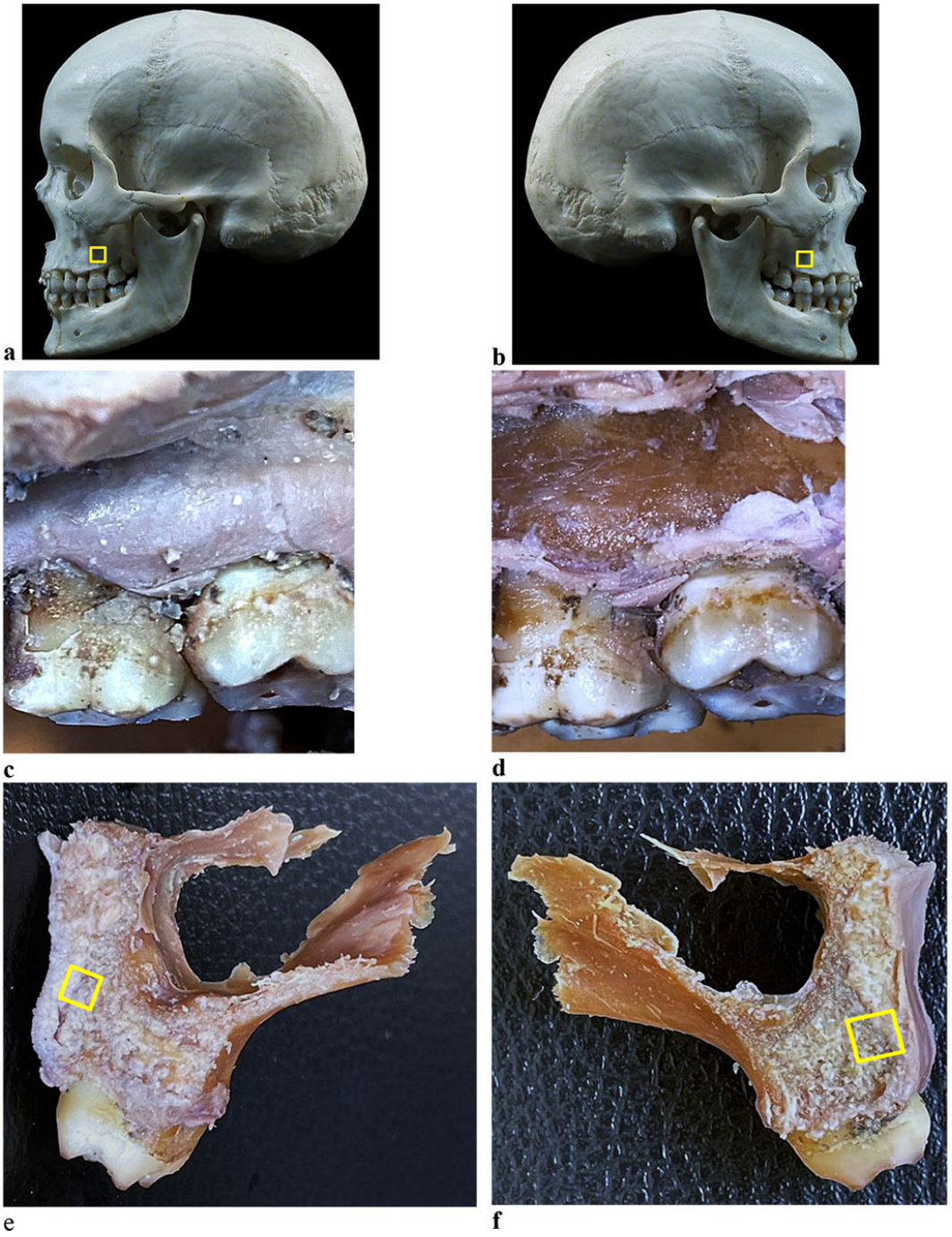

Figure 2. Bone biopsy specimen from the distal alveolar process of the maxilla with preserved dentition: a, b - areas for taking bone preparations on the skull; anatomical preparation before (c) and after (d) separation of the muco-periosteal flap in the area of the 26th tooth; areas for taking a bone preparation on the maxillary first molar segment (e - 16 tooth, f - 26 tooth).

For morphology examination of the periodontal ligament at various levels of the root, 6 maxillary segments of the medial incisors and 6 maxillary segments of the first molars of the upper jaw were obtained from the vestibular, oral, medial and distal surfaces (Fig. 3,4).

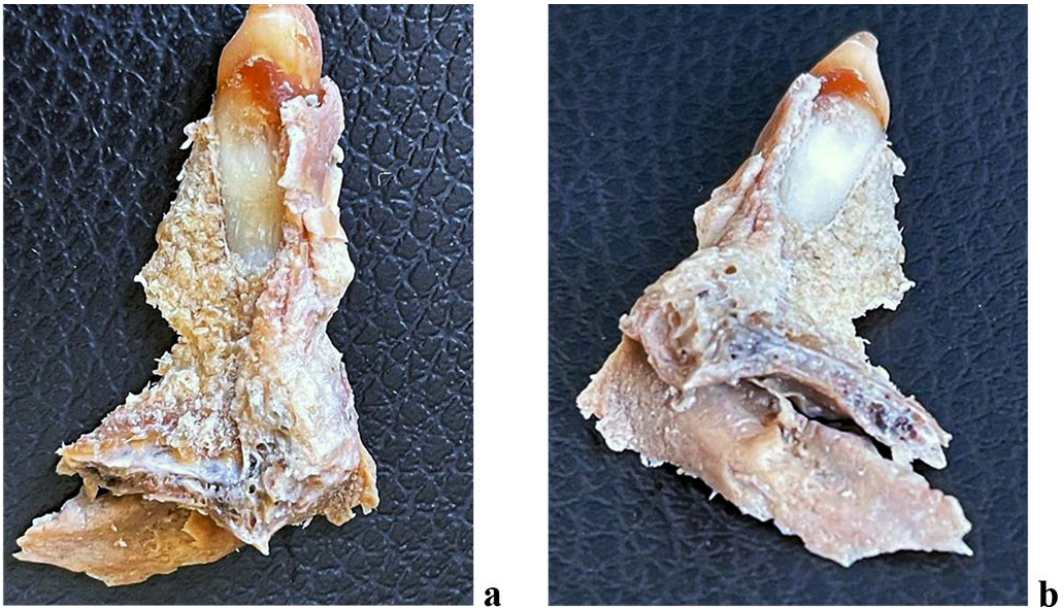

Figure 3. The dentition segment of the medial incisor of the maxilla: a - medial surface; b - distal surface.

Figure 4. Maxillary segment of the maxillary first molar: a - vestibular surface; b - oral surface; c - medial surface; d - distal surface; e, f - projection from the maxillary sinus side.

The material was fixed in a 10% solution of neutral buffered formalin for 48 hours. Once the fixation completed, decalcification was carried out in a 25% Trilon B solution of organic acid, with further dehydration in isopropanol of ascending concentration employing a Leica TR1020 automatic carousel-type tissue processor (Leica Microsystems, Nussloch, GmbH) (Fig. 5), with further pouring into paraffin (Histomix, Biovitrum), with the filling system applied.

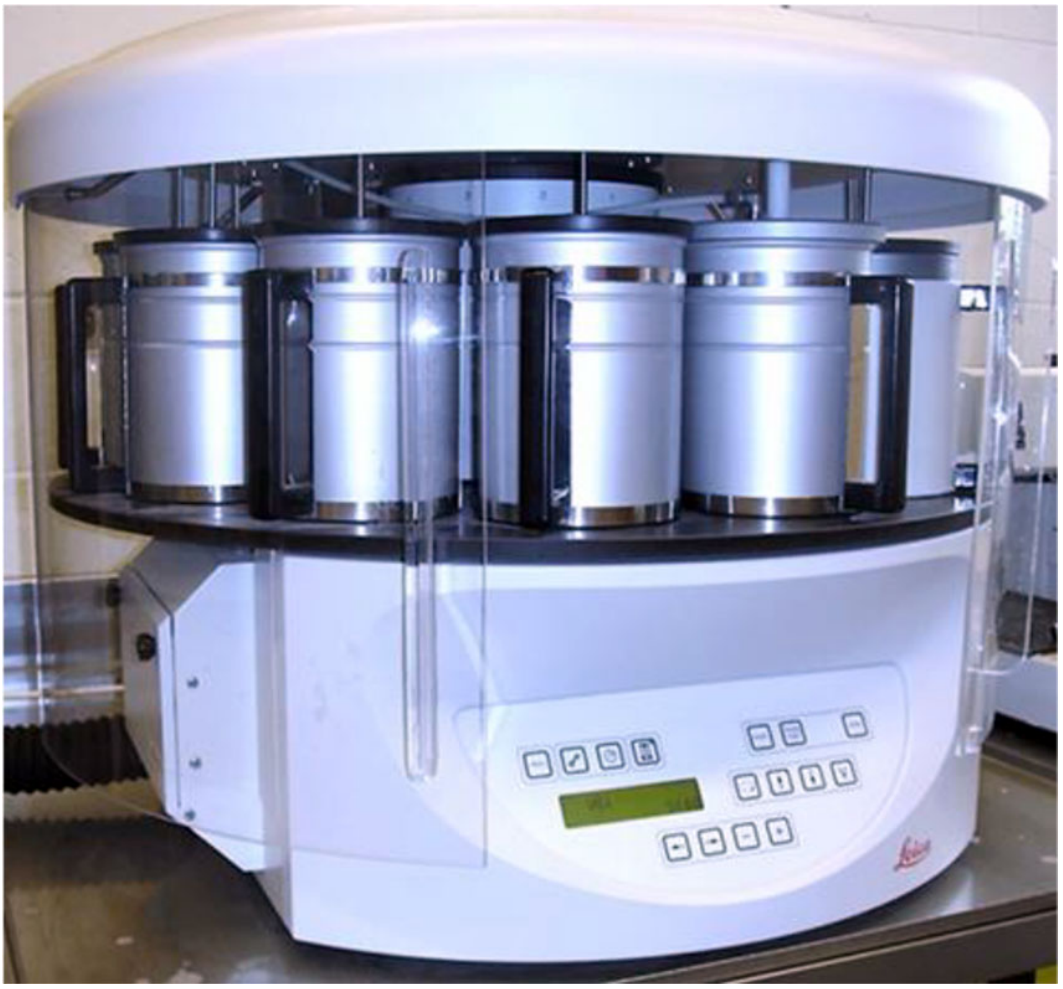

Figure 5. Leica TP1020 Automatic system for tissue histological processing.

The processing and pouring into paraffin finished, serial sections were produced (thickness – 5-7 microns) with a Leica RM2235 manually controlled rotary microtome (Leica Microsystems, Germany) (Fig. 6).

Figure 6. Leica RM2235 manually controlled rotary microtome.

The paraffined sections were stained with hematoxylin and eosin (Biovitrum, Russia) and picrofuxin (by Van Gieson), while using a Raffaello staining unit (DIAPATH, S.p.A., Italy). The histological examination of the samples was performed using a Leica DM2500 hardware and software set (Leica Microsystems; magnification: ×20 – × 1000) (Fig. 7).

Figure 7. Leica DM2500 lab microscope.

The morphometric parameters measurements for quantitative assessment of the maxillary alveolar process microarchitectonics and angioarchitectonics were carried out in the ImadgeJ software (National Institutes of Health, USA) on a Leica DM2500 set. While studying the sections, the following was the focus within vision: the number of vessels per 1.0 mm2; the size of blood vessels (diameter); the thickness of the blood vessel walls. At magnification (×200), each histological slice in six areas of vision (the image size being 100×75 microns; area: 7.5 mm2) had the following parameters identified in the general data array: the area of blood vessels; the area of lymphatic vessels; the area of loose connective tissue; the area of dense connective tissue.

The maxillary segment sections of the medial incisors and the first molars were prepared in a horizontal plane at the level of the gingival, middle and apical parts of the root (Fig. 8-10).

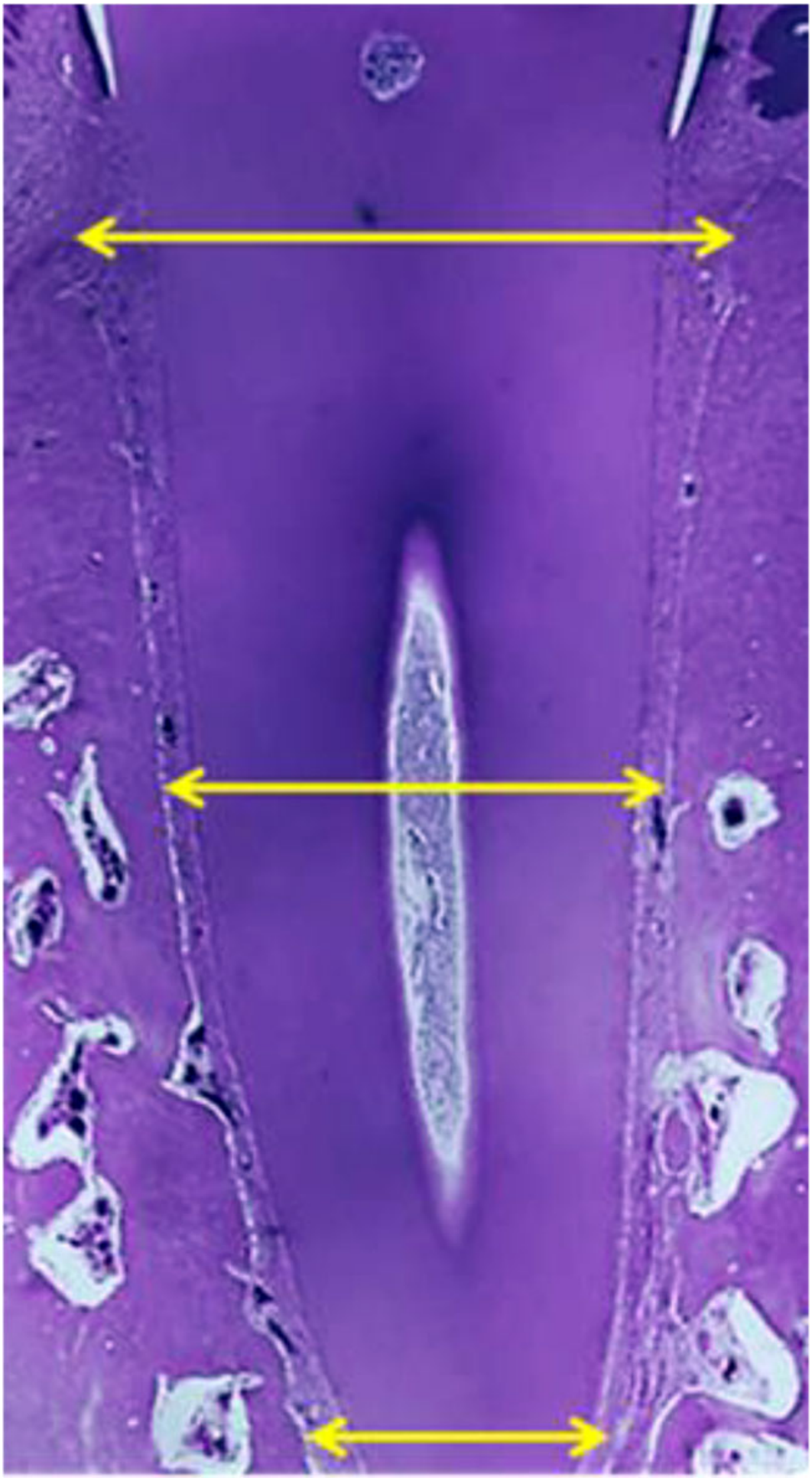

Figure 8. Histological sample of the maxillary segment of the maxillary central incisor with the

root examination zones marked: gingival, middle, apical (×20, hematoxylin-eosin stain).

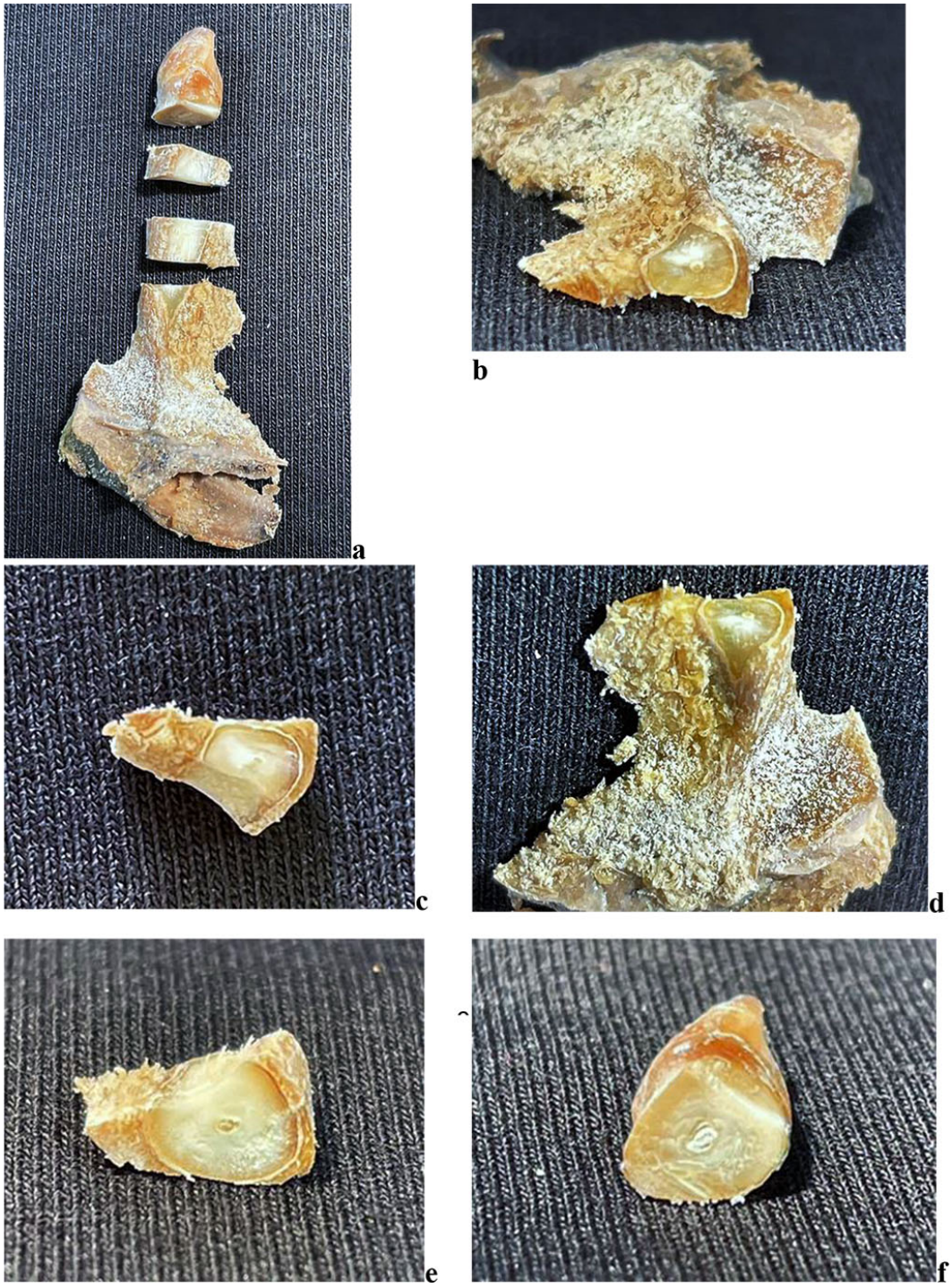

Figure 9. Maxillary segment of the maxillary central incisor with periodontal ligament study areas: a - general view of the maxillary segment; b, c - apical part of the maxillary segment; d - middle part of the maxillary segment; e - gingival part of the maxillary segment; f - crown of the tooth.

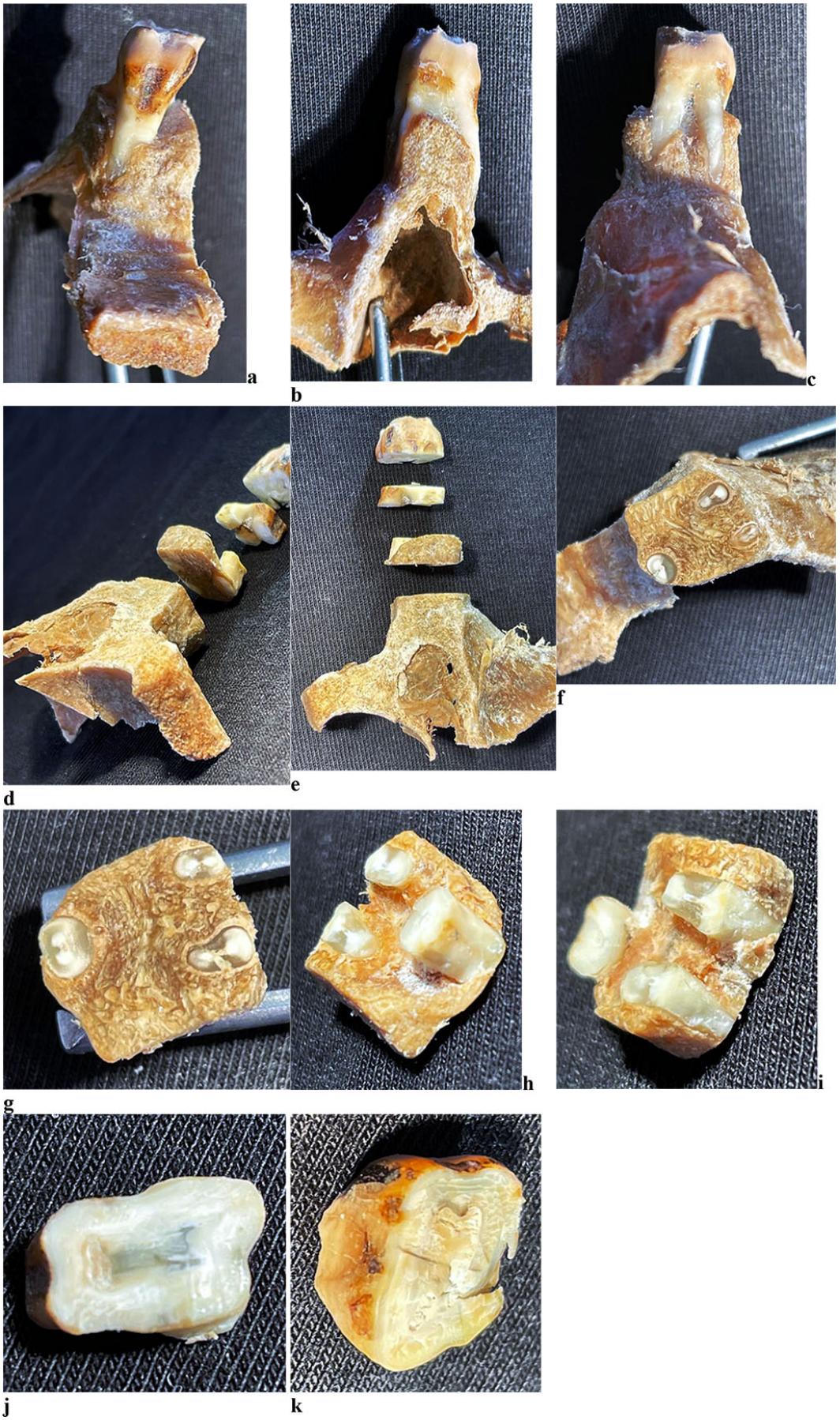

Figure 10. Maxillary segment of the maxillary first molar with periodontal ligament study areas: maxillary segment from oral surface (a), medial surface (b), distal surface (c); d, e - general view of maxillary segment; f, g - apical part of maxillary segment; h, i - middle part of maxillary segment; j - gingival part of maxillary segment; k - crown of tooth.

The statistical data processing was done using the nonparametric Mann-Whitney criterion on the Microsoft

Windows 10.0 operating system in the Microsoft Excel 2019, Statistica 12.0 software package (StatSoft Inc., USA).

RESULTS AND DISCUSSION

Given their histological structure, the jaw bones can be classified as lamellar ones, which means they consist of bone plates tightly adjacent to one another. The maxillary alveolar process includes the alveolar bone itself (the alveoli walls) and the supporting alveolar bone. The proper alveolar bone is a thin (0.1-0.4 mm) bone plate surrounding the tooth root and is the spot of periodontal fibers attachment. The center of the osteon has a canal hosting vessels and vegetative nerve fibers. On the side of the periosteum and bone marrow, there are internal and external general bone plates to be observed covering the entire bone. The outer bone plate has holes – Volkmann canals, which serves the way for vessels and vegetative nerve fibers to penetrate into the Haversian canals. Also, there are piercing bundles of collagen fibers running from the periosteum, which are pointed towards the bone (Sharpey's fibers). Sharpey's periodontal fibers ensure strong periosteum-to-bone attachment. The supporting alveolar bone includes a compact bone which shapes the outer and the inner walls of the alveolar process, as well as a spongy bone filling the spaces between the alveolar process walls and the alveolar bone itself. The cortical plates of the alveolar process run on turning into respective plates of the upper jaw body, while reaching their top thickness in the buccal surface of the molars. The cortical plates of the alveolar process are made up of longitudinal plates and osteones. The spongy bone is a mass of anastomosing trabeculae whose distribution matches the direction of the chewing force. At the alveoli lateral walls, the trabeculae feature mainly horizontal orientation, and vertical – at the bottom of the alveoli. The number of trabeculae varies in different parts of the alveolar process. The spongy bone makes up the inter-root and interdental septa containing vertical feeding canals containing nerves, blood and lymph vessels. Between the bone trabeculae there are bone marrow spaces filled with yellow bone marrow.

The maxillary periosteum has arteries running as part of the neurovascular bundles. They enter the outer layer from a large arterial trunk, and as they go on deepening into the inner layer of the periosteum, there are thinner arterial branches running off at different angles. The outer and inner layers in the periosteum have arterial networks formed by vascular branches, which are located above the nerve plexuses. The upper jaw periosteum features a radial arrangement of neurovascular bundles, which – 3-4 of them all together – enter the periosteum from a. infraorbitalis and n. infraorbitalis. Furter on, the neurovascular bundles are running to the lower edge of the orbit, the pear-shaped foramen, the alveolar process and to the zygomatic-alveolar ridge, where they anastomose with the posterior upper alveolar branches of the arteries and nerves.

The microarchitectonics of the maxillary alveolar process in the frontal part with preserved (intact) dentition appears as a typical thin-fiber lamellar bone tissue. The main structural component of lamellar bone tissue is the bone plate, which consists of osteocytes and intercellular substance with an insignificant amount of the basic substance (Fig. 11.a). The bone plates feature a longitudinal orientation. Osteocytes are star-shaped. The nucleus of osteocytes is located in the central part of the cells. Osteocytes are oriented mainly along the course of the bone plates (Fig. 11.b). Angioarchitectonics of the maxillary alveolar process in the frontal part with preserved dentition is made up of tubular structures, mainly running perpendicular to the bone surface, with a large number of anastomoses (Fig. 11.c). There is a moderate degree of bone vascularization to be noted. Cross-section of arterial vessels reveals their rounded shape and a thin wall, the diameter of the arteries being 3-4 times as small as the diameter of the veins (Fig. 11.d).

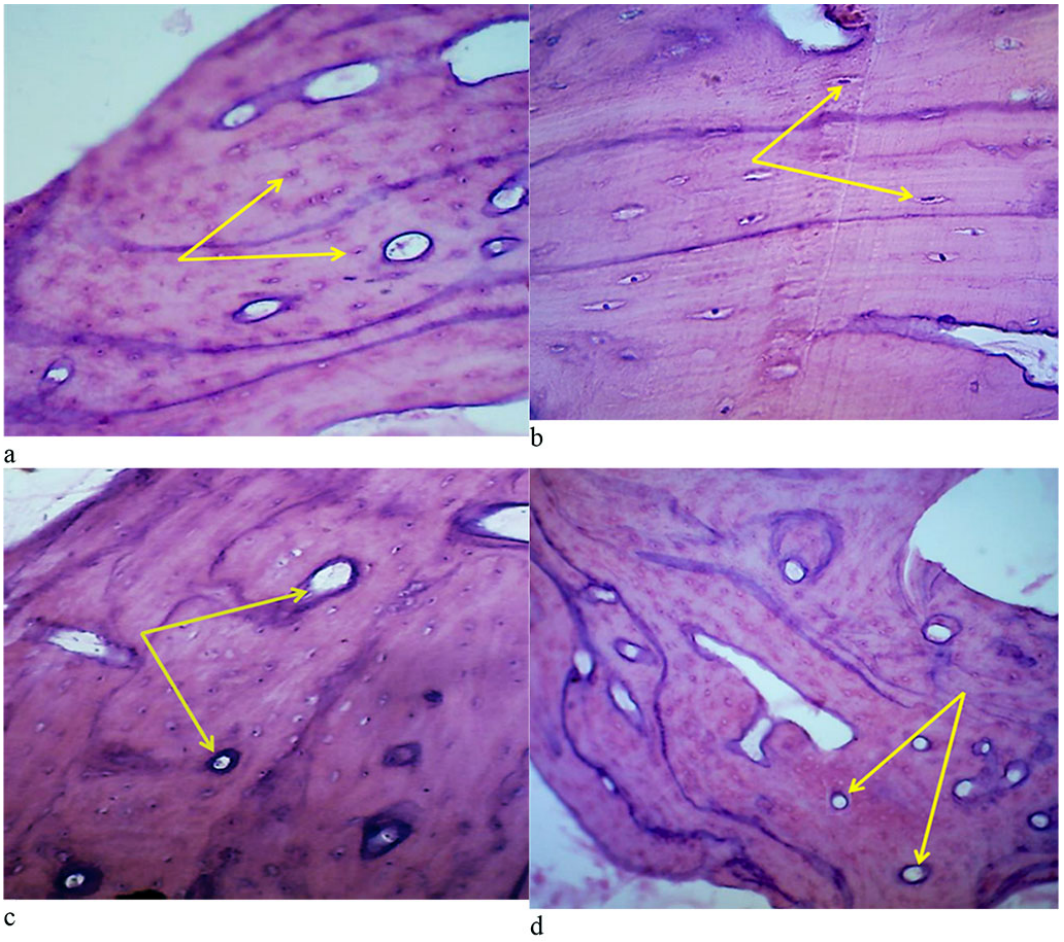

Figure 11. Bone biopsy from the frontal part of the maxillary alveolar process with intact dentition: a – microarchitectonics of the maxillary alveolar process in the projection of the 11th tooth (×200, hematoxylin-eosin staining, osteocytes are indicated by arrows); b – microarchitectonics of the maxillary alveolar process in the projection of the 21st tooth (×800, hematoxylin-eosin staining, arrows indicate osteocytes); b – angioarchitectonics of the maxillary alveolar process in the projection of the 11th tooth (×200, hematoxylin-eosin stain, arrows indicate blood vessels); d – angioarchitectonics of the maxillary alveolar process in the projection of the 21st tooth (×200, hematoxylin-eosin staining, blood vessels are indicated by arrows).

The microarchitectonics of the maxillary alveolar process in the distal part with preserved (intact) dentition is basically no different if compared to the morphology of bone tissue in the projection of the frontal group of teeth. The orientation of the bone plates runs along concentric circles, which are located around the Haversian canals (Fig. 12).

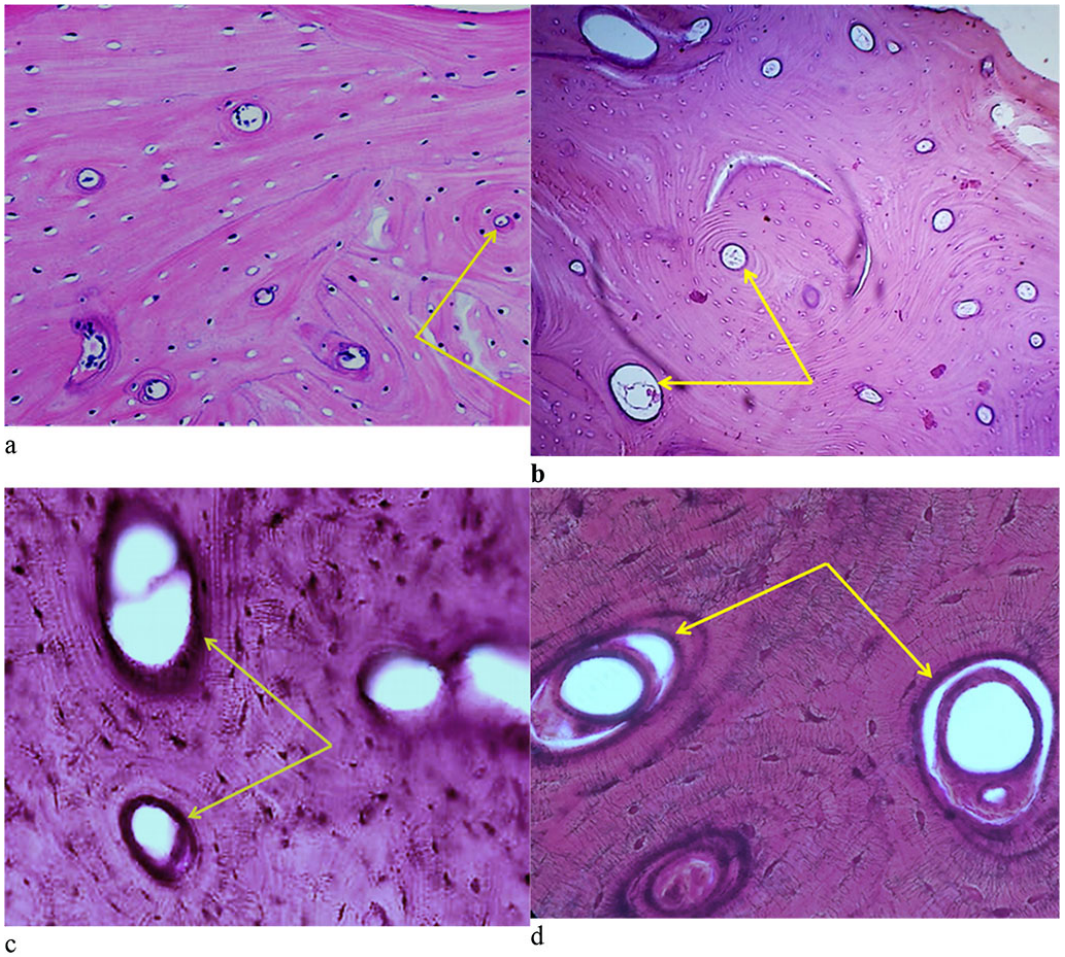

Figure 12. Bone biopsy from the distal part of the maxillary alveolar process with preserved dentition: a – microarchitectonics of the maxillary alveolar process in the projection of the 16th tooth (×100, hematoxylin-eosin staining, the arrows indicate the Haversian canals); b – microarchitectonics of the maxillary alveolar process in the projection of the 26th tooth (×200, hematoxylin-eosin staining, arrows indicate the Haversian canals); c – microarchitectonics of the maxillary alveolar process in the projection of the 16th tooth (×800, hematoxylin-eosin staining, arrows indicate the Haversian canals); d – microarchitectonics of the maxillary alveolar process in the projection of the 26th tooth (×1000, hematoxylin-eosin color, arrows indicate the Haversian canals).

The cross section of the arteries reveals their rounded shape, the walls being thin. The veins lumen seen on the cross section is of an oval or rounded shape, whereas the diameter of the arteries is 3-4 times as small as the diameter of the veins (Fig. 13).

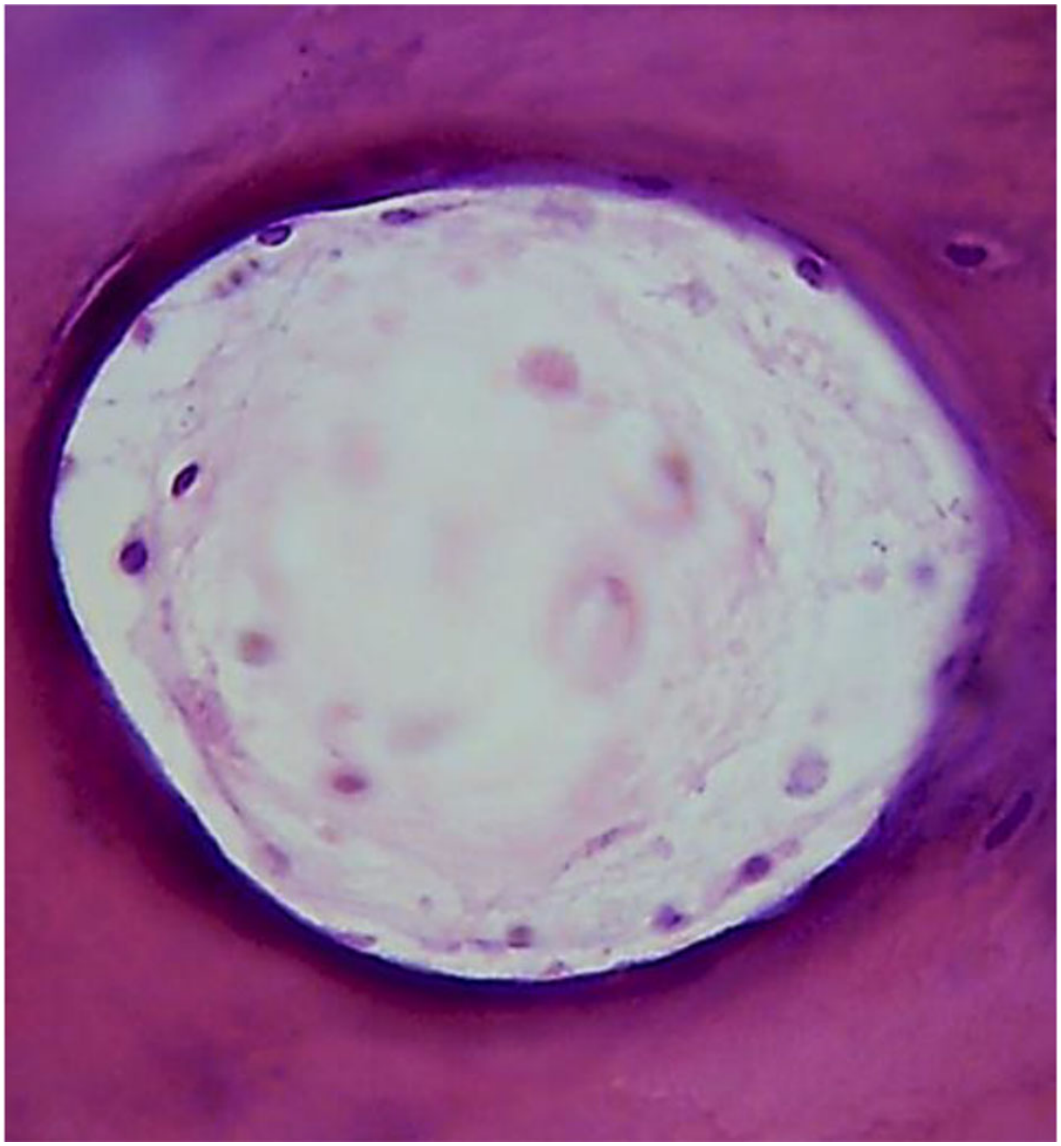

Figure 13. Morphological presentation of the maxillary alveolar process artery in the projection of the 21st tooth with preserved dentition (×800, hematoxylin-eosin stain).

The angioarchitectonics of the maxillary alveolar process in the distal part with preserved dentition features arterial and venous vessels, as well as vessels of the microcirculatory bed, which make up numerous anastomoses. In ⅓ of all most cases, the anastomoses are oriented in the same plane with the network-like structures, whereas in the remaining ⅔ of the cases they are located parallel to the bone beams (Fig. 14).

Figure 14. Angioarchitectonics of the maxillary alveolar process in the distal part with preserved dentition: a –the microcirculatory bed vessels, net-shaped, in the projection of the 26th tooth (×400, hematoxylin-eosin staining); b – the microcirculatory bed vessels, running parallel to the bone beams in the projection of the 26th tooth (×800, hematoxylin-eosin staining).

Tables 1-2 contain the values of quantitative indicators for the maxillary alveolar process vascular system, preserved dentition.

Table 1. Morphometric parameters of the maxillary alveolar process vascular system in the frontal part, (M±m)

Metric parameters	Tooth 11	Tooth 21	p
Vessels per 1 mm^2	22.87 ± 2.08	22.41 ± 1.76	p≤0.01
Size of blood vessels (center), micron	26.06 ± 3.17	25.34 ± 2.45	p≤0.05
Vessel wall thickness, micron	1.43 ± 0.09	1.48 ± 0.12	p≤0.01

Table 2. Morphometric parameters of the maxillary alveolar process vascular system in the distal part, (M±m)

Metric parameters	Tooth 16	Tooth 26	p
Vessels per 1 mm^2	25.02 ± 2.69	23.94 ± 1.88	p≤0.01
Size of blood vessels (center), micron	26.14 ± 2.93	25.72 ± 2.31	p≤0.05
Vessel wall thickness, micron	1.54 ± 0.14	1.50 ± 0.11	p≤0.01

The average number of vessels with preserved dentitions on an area of 1 mm^2 in the projection of the 11th tooth was 22.87 ± 2.08; in the projection of the 21st tooth – 22.41 ± 1.76; in the projection of the 16th tooth – 25.02± 2.69; in the projection of the 26th tooth – 23.94± 1.88, with no statistically significant difference identified between the indicators in the frontal and distal sections (p≤0.01).

The average diameter of vessels with intact dentition in the projection of the 11th tooth was 26.06 ± 3.17 microns; in the projection of the 21st tooth – 25.34 ± 2.45 microns; in the projection of the 16th tooth – 26.14 ± 2.93 microns, in the projection of the 26th tooth – 25.72 ± 2.31 microns, no statistically significant difference detected between the values in the frontal and distal sections ($p \leq 0.05$).

The average wall thickness with preserved dentition rows in the projection of the 11th tooth was 1.43 ± 0.09 microns; in the projection of the 21st tooth – 1.48 ± 0.12 microns; in the projection of the 16th tooth – 1.54 ± 0.14 microns, in the projection of the 26th tooth – 1.50± 0.11 microns, while the statistically significant difference between the indicators in the frontal and distal set ($p \leq 0.01$).

As the results of histological studies focusing on the periodontal ligament at the level of the gingival, middle and apical parts of the root show, periodontal fibers are well visualized, and they border on one side with the tooth cement, while with lamellar bone tissue – on the other. The lamellar bone has individual osteons and develops outgrowing spins towards the periodontium. The periodontal ligament appears as a thick bundles of collagen fibers. Bundles of periodontal collagen fibers have a radial direction, their one end embedded in the cement (dental fibers), the other – in the alveolar bone outgrowths (alveolar fibers). The thickness of the terminal sections (Sharpey's) of fibers in the bone is 10-20 microns, in the cement – 3-5 microns. Periodontal collagen fibers with a diameter of 50-60 microns feature a wave-like course of fibers to ensure micro-movement of the tooth in the alveolus (Fig. 15).

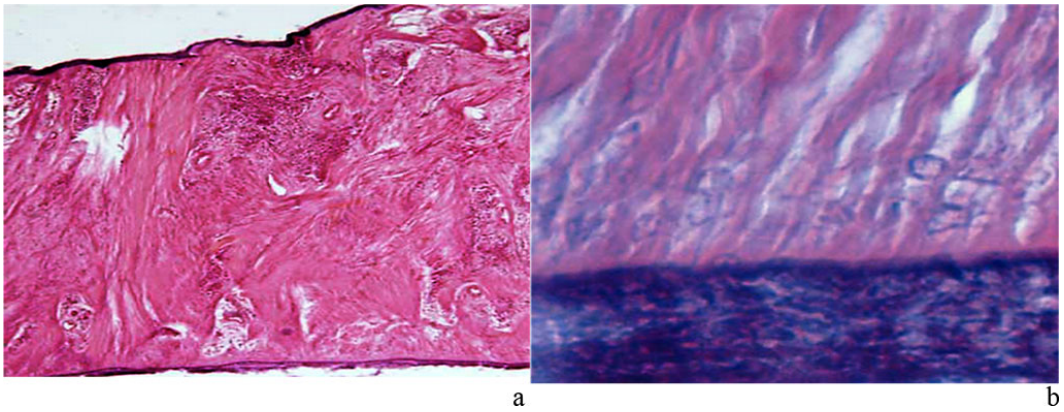

Figure 15. Periodontal ligament of the maxillary segment of the first molar: a – dense fibrous connective tissue (×400, hematoxylin-eosin staining); b – zone of dense fibrous connective tissue penetrating cement (×1000, hematoxylin-eosin staining).

Besides, there are bundles of collagen fibers branching off the bone tissue plate, which have a tangential (longitudinal) direction. A loose fibrous unformed connective tissue is located between the bundles of collagen fibers, while its volume is much lower than that of dense connective tissue. The cellular composition of the periodontium features the following elements: fibroblasts (ab. 50%), which make up a single three-dimensional network by means of desmosomes, slit and dense connections; poorly differentiated polypotent cells located near small blood vessels; osteoblasts located on the surface of the alveolar process; cementoblasts at the periodontium facing the tooth root; osteoclasts and cementoclasts located in lacunae on the surface of the bone and root of the tooth; macrophages, mast cells and leukocytes localized in the interstitial connective tissue of the periodontium; epithelial remnants of Malassez located at the neck and tip of the tooth root (Fig. 16).

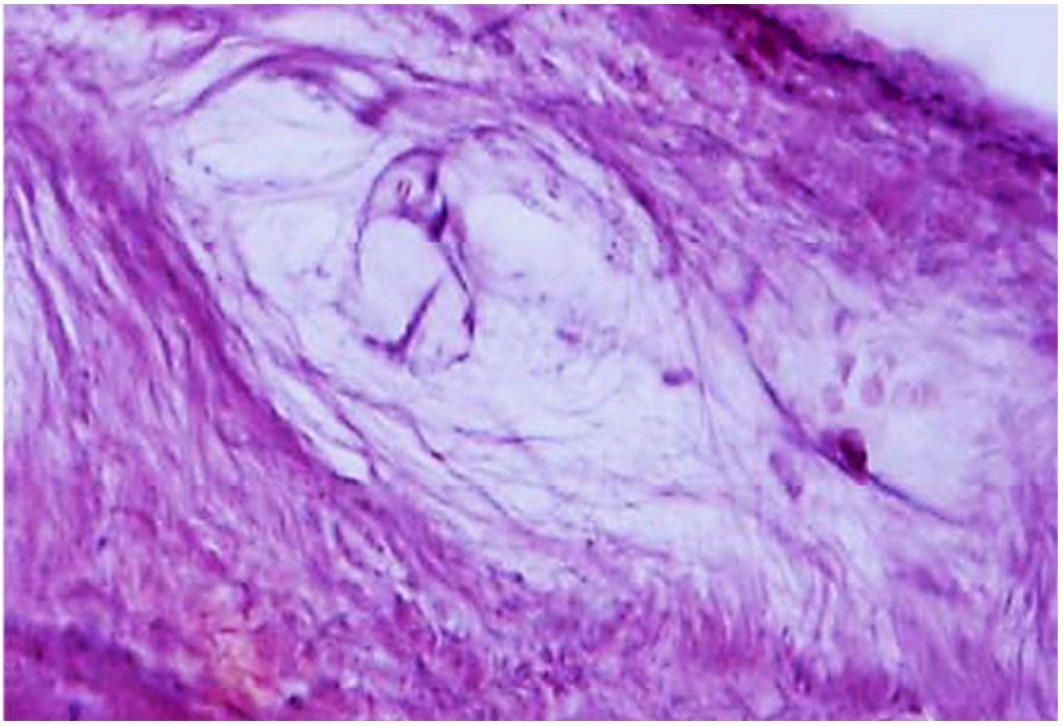

Figure 16. Periodontal ligament of the maxillary medial incisor dentoalveolar segment. Loose fibrous unformed connective tissue and periodontal cellular elements (×1000, hematoxylin-eosin stain).

Periodontal angioarchitectonics is numerous blood vessels of various diameters and types – from small arteries, arterioles and hemocapillaries to veins. The main sources of periodontal blood supply are include aa. alveolares superiores anteriores and a. alveolaris superior posterior. Blood supply, venous and lymphatic outflow in the periodontium features the following: part of the hemocapillaries have a fenestrated endothelium; numerous anastomoses between arterial and venous vessels; poor development of the lymphatic vessel system; numerous anastomoses between periodontal blood vessels and gum vessels, bone and the jaw oblique spaces (Fig. 17).

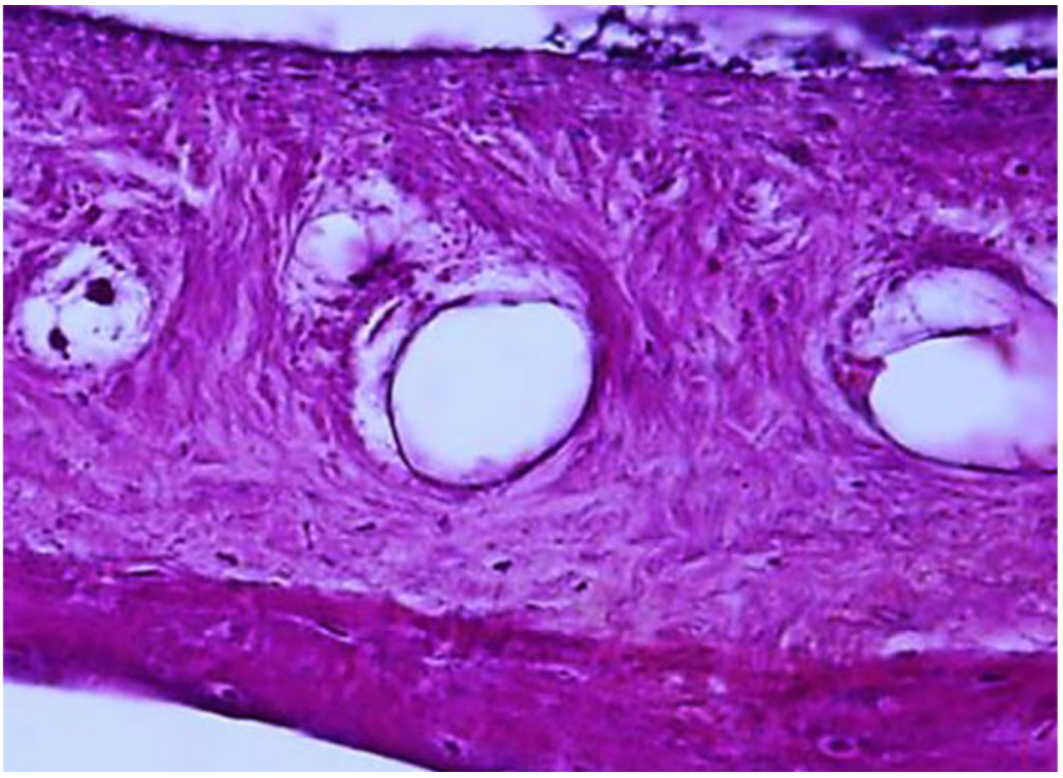

Figure 17. Periodontal ligament of the dentoalveolar segment of the maxillary medial incisor. Multiple anastomoses between arterial and venous vessels (×400, hematoxylin-eosin stain).

Lymphatic vessels have a very thin wall, which incorporates individual nuclei of endothelial cells, while there are no typically shaped blood elements in the vessel lumens. Lymphatic vessels are mainly located near the cement and the bone tissue. The lymphatic vessels orientation in the middle part of the root is longitudinal, while at the apex and gums – circular. The main (amorphous) substance of the periodontium is a highly viscous gel, whereas a significant volume of the tissue fluid acts as a cushion in case of a loading stress.

Tables 3-5offer a look at the results of quantitative analysis focusing on the structural elements of the periodontal medial incisors at different root levels.

Table 3. Histological indicators for the structural elements of the medial incisors periodontium at the level of the gingival part of the root from different sides (area percentage as per each parameter, six fields within vision), (M ±m), (%)

Periodontium structural elements	Share in total data array			
	Vestibular surface	Oral surface	Medial surface	Distal surface
Dense connective tissue	57.82 ± 5.44	66.98 ± 4.85*	65.49 ± 5.57*	63.75 ± 4.79*
Loose connective tissue	26.39 ± 4.02	19.73 ± 3.26*	22.72 ± 3.48*	24.28 ± 3.91*
Blood vessels	7.91 ± 0.53	9.02 ± 0.41*	6.93 ± 0.35*	6.56 ± 0.44*
Lymphatic vessels	7.88 ± 0.46	4.27 ± 0.18*	4.86 ± 0.21*	5.41 ± 0.29*

Note: statistically significant compared with the share of structural elements on the vestibular surface (p ≤0.05).

Table 4. Histological indicators for the structural elements of the medial incisors periodontium at the level of the middle part of the root from different sides (area percentage as per each parameter, six fields within vision), (M ±m), (%)

Periodontium structural elements	Share in total data array			
	Vestibular surface	Oral surface	Medial surface	Distal surface
Dense connective tissue	74.20 ± 5.63	74.91 ± 5.09*	69.19 ± 4.77*	67.26 ± 4.21*
Loose connective tissue	13.07 ± 0.89	11.87 ± 1.02*	13.93 ± 0.96*	17.94 ± 2.36*
Blood vessels	5.39 ± 0.56	5.18 ± 0.37*	6.07 ± 0.41*	5.49 ± 0.28*
Lymphatic vessels	7.34 ± 0.43	8.04 ± 0.52*	10.81 ± 0.84*	9.31 ± 0.65*

Note: statistically significant compared with the share of structural elements on the vestibular surface (p ≤0.05).

Table 5. Histological indicators for the structural elements of the medial incisors periodontium at the level of the apical part of the root from different sides (area percentage as per each parameter, six fields within vision), (M ±m), (%)

Periodontium structural elements	Share in total data array			
	Vestibular surface	Oral surface	Medial surface	Distal surface
Dense connective tissue	73.08 ± 4.07	68.84 ± 4.69*	64.72 ± 3.83*	62.87 ± 4.05*
Loose connective tissue	13.23 ± 1.24	17.92 ± 0.76*	23.30 ± 3.99*	19.96 ± 1.83*
Blood vessels	7.95 ± 0.49	6.21 ± 0.38*	5.37 ± 0.27*	5.74 ± 0.32*
Lymphatic vessels	5.74 ± 0.63	7.03 ± 0.52*	6.61 ± 0.58*	11.43 ± 0.71*

Note: statistically significant compared with the share of structural elements on the vestibular surface (p ≤0.05).

A quantitative assessment of the medial incisors periodontal structures show that the area of dense connective tissue exceeds (statistically significant) the area of loose connective tissue regardless of the level of the tooth root part, whereas the ratio of the studied parameters varies on different tooth surfaces. The area of dense connective tissue of the medial incisors gingival part on the oral surface (66.98 ±4.85%) is significantly (p≤0.05) larger than that on the vestibular (57.82±5.44%) part, while the differences between the medial (65.49± 5.57%) and distal (63.75±4.79%) surfaces are not significant. There has been an inverse relationship identified with respect to the area of loose connective tissue – in the gingival part, its share is greater on the vestibular surface (26.39±4.02%) than on the oral part (19.73±3.26%) (p≤0.05), the differences between the medial (22.72±3.48%) and distal (24.28±3.91%) surfaces being not reliable.

Subject to the position of the medial incisors biomechanical model, the area of *the periodontal ligament compression* at the gingival root part level is the vestibular surface, while the *periodontal ligament stretching* area is the oral surface. In the middle part of the medial incisors root, the largest area of dense connective tissue was detected on the vestibular (74.20±5.63%) and oral (74.91±5.09%) surfaces, combined with the smallest share of loose connective tissue (13.07± 0.89% and 11.87± 1.02%, respectively). Experts claim that the median area of the root is the greatest resistance area, where the gravity forces in case of chewing load are located in the middle third. An inverse relationship has been identified in the root apical part. The area of medial incisors dense connective tissue in the apical part on the oral surface (68.84 ±4.69%) is significantly (p≤0.05) smaller than on the vestibular (73.08± 4.07%) part, while the differences between the medial (64.72± 3.83%) and distal (62.87± 4.05%) surfaces are not significant.

The area of loose connective tissue in the apical part is greater on the oral surface (17.92±0.76%) than on the vestibular (13.23±1.24%) (p≤0.05), and on the medial surface (23.30±3.99%) it is greater than on the distal (19.96±1.83%) (p≤0.05) one. The specific share of periodontium blood and lymphatic vessels of medial incisors differs significantly if measured on different sides of the root. The largest specific area of blood vessels was observed in the gingival part on the oral surface (9.02±0.41%) and in the apical part on the vestibular surface (7.95± 0.49%) of the root, which corresponds to the *periodontal ligament compression* zones under biomechanical loads. Notable is that the specific share of lymphatic vessels at the level of the gingival part of the root with oral (4.27±0.18%), medial (4.86±0.21%) and distal (5.41±0.29%) surfaces is significantly (p≤0.05) lower than on similar surfaces at the level of the middle part of the root (8.04±0.52%, 10.81±0.84% and 9.31±0.65% , respectively) and the apical part of the root (7,03±0,52%, 6,61±0,58% and 11.43± 0.71%, respectively).

Table 6-8 shows the data obtained through a quantitative analysis of the structural elements of the first molars periodontium at different levels of the root.

Table 6. Histological indicators for the structural elements of the first molars periodontium at the level of the gingival part of the root from different sides (area percentage as per each parameter, six fields within vision), (M ± m), (%)

Periodontium structural	Share in total data array

elements	Vestibular surface	Oral surface	Medial surface	Distal surface
Dense connective tissue	52.04 ± 3.86	61.18 ± 5.03*	49.24 ± 4.78*	62.93 ± 6.14*
Loose connective tissue	34.59 ± 2.37	27.33 ± 3.42*	40.78 ± 5.19*	26.61 ± 4.04*
Blood vessels	7.62 ± 0.41	6.13 ± 0.39*	5.87 ± 0.32*	5.52 ± 0.27*
Lymphatic vessels	5.75 ± 0.28	5.36 ± 0.21*	4.11 ± 0.24*	4.94 ± 0.35*

Note: statistically significant compared with the share of structural elements on the vestibular surface (p ≤0.05).

Table 7. Histological indicators for the structural elements of the first molars periodontium at the level of the middle part of the root from different sides (area percentage as per each parameter, six fields within vision), (M ±m), (%)

Periodontium structural elements	Share in total data array			
	Vestibular surface	Oral surface	Medial surface	Distal surface
Dense connective tissue	59.96 ± 4.97	77.53 ± 4.16*	63.06 ± 5.27*	70.11 ± 4.68*
Loose connective tissue	30.14 ± 3.21	13.35 ± 1.38*	26.85 ± 3.72*	21.27 ± 2.86*
Blood vessels	6.21 ± 0.36	4.84 ± 0.22*	5.73 ± 0.32*	3.89 ± 0.25*
Lymphatic vessels	3.69 ± 0.19	4.28 ± 0.26*	4.36 ± 0.34*	4.73 ± 0.31*

Note: statistically significant compared with the share of structural elements on the vestibular surface (p ≤0.05).

Table 8. Histological indicators for the structural elements of the first molars periodontium at the level of the apical part of the root from different sides (area percentage as per each parameter, six fields within vision), (M ±m), (%)

Periodontium structural elements	Share in total data array			
	Vestibular surface	Oral surface	Medial surface	Distal surface
Dense connective tissue	62.73 ± 4.28	61.14 ± 4.77*	69.41 ± 5.02*	68.96 ± 4.34*
Loose connective tissue	25.79 ± 2.86	23.47 ± 3.05*	21.78 ± 3.99*	19.92 ± 2.18*
Blood vessels	6.63 ± 0.33	7.46 ± 0.41*	3.92 ± 0.21*	5.08 ± 0.26*

Lymphatic vessels	4.85 ± 0.17	7.93 ± 0.38*	4.89 ± 0.29*	6.04 ± 0.34*

Note: statistically significant compared with the share of structural elements on the vestibular surface (p ≤0.05).

A quantitative analysis of the first molars periodontium structures suggests that the area of dense connective tissue is also statistically significantly above the area of loose connective tissue at all levels of the tooth root part.

The area of the first molars dense connective tissue in the gingival part on the distal surface (62.93±6.14%) is statistically significantly (p≤0.05) larger than on the medial (49.24±4.78%), and on the oral surface (61.18±5.03%) it is significantly (p≤0.05) greater than on the vestibular (52.04±3.86%) one. There has been an inverse relationship revealed with respect to the loose connective tissue area – in the gingival part, its share is greater on the medial surface (40.78±5.19%) than on the distal one (26.61±4.04%) (p≤0.05), and on the vestibular surface (34.59±2.37%) it exceeds significantly (p≤0.05) the similar indicator pertaining to the oral surface (27.33±3.42%).

As the position of the first molars biomechanical model shows, the *periodontal ligament compression* areas at the level of the gingival part of the root are the vestibular and medial surfaces, while the *periodontal ligament stretching* areas are the distal and oral surfaces. In the middle part of the first molars root, the largest area of dense connective tissue is located on the oral (77.53± 4.16%) and distal (70.11± 4.68%) surfaces, combined with the smallest proportion of loose connective tissue (13.35± 1.38% and 21.27± 2.86%, respectively). It has been reliably proven that the middle third of the first molars root (root bifurcation area) is the area of maximum resistance, with the concentration of gravity to be observed there at chewing load.

In the apical part of the first molars root, the area of dense connective tissue on the medial (69.41±5.02%) and distal (68.96±4.34%) surfaces exceeds slightly the area on the vestibular (62.73±4.28%) and oral (61.14±4.77%) surfaces, while the area of loose connective tissue on the vestibular (25.79±2.86%) and oral (23.47±3.05%) surfaces is not significantly above the specific area of loose connective tissue on the medial (21.78±3.99%) and distal (19.92±2.18%) surfaces. The specific share of blood and lymphatic vessels of the first molars periodontium varies significantly if measured on different sides of the root. The largest area taken by blood vessels was observed on the vestibular surface in the gingival part (7.62± 0.41%) and at the level of the middle third of the root (6.21± 0.36%), as well as on the oral surface (7.46± 0.41%) in the root apical part, which corresponds to the *periodontal ligament compression* area under biomechanical loads. The variability limits of the specific share of periodontal lymphatic vessels on different surfaces and levels of the first molars root differ slightly from similar quantitative indicators of blood vessels.

CONCLUSIONS

1. As the histological studies show, the microarchitectonics of the maxillary alveolar process with preserved dentition features a typical thin-fiber lamellar bone tissue. The orientation of the bone plates in the frontal part is longitudinal, whereas in the distal part it runs along concentric circles located around the Haversian canals. Osteocytes are of a stellate shape, the nucleus located in the central part of the cells. Osteocytes are oriented mainly along the course of the bone plates.
2. The angioarchitectonics of the maxillary alveolar process with preserved dentition features tubular structures, mainly running perpendicular to the bone surface, with a large number of anastomoses. Bone vascularization is moderate. A cross-section of arterial vessels is rounded, with thin walls, while the diameter of the arteries is 3-4 times as small as the diameter of the veins.
3. The data of a morphometric analysis focusing on the vascular system of the maxillary alveolar process with preserved dentition show that in the frontal section, the number of vessels per 1 mm^2 is 22.41± 1.76 - 22.87± 2.08; in the distal section – 23.94± 1.88 - 25.02± 2.69 (p≤0.01); the average diameter of vessels in the frontal section is 25.34 ±2.45 microns - 26.06±3.17 microns; in the distal section – 25.72±2.31 microns - 26.14±2.93 microns (p≤0.05); the average wall thickness in the frontal section is 1.43±0.09 microns - 1.48±0.12 microns; in the distal section – 1.50±0.11 microns - 1.54±0.14 microns (p≤0.01).
4. The identified quantitative data of morphometric parameters of the maxillary alveolar process vascular system, in case of preserved dentition, are the most important diagnostic criteria in detecting the severity of vascular issues. Morphometric evaluation criteria employed along with the analysis of clinical manifestations can be a reasonable option for monitoring the early stages of morphofunctional disorders, as well as for evaluating the treatment effectiveness.
5. The spongy substance of the incisor-maxillary segments of the upper jaw includes long beams of

bone running into the palatine and alveolar processes. The cells of the spongy substance are oval, running along the course of the beams. The width of the periodontal gap in the gingival part can be up to 0.2 mm, and in the apical part – 0.4 mm.

6. The maxillary palatine process at the level of the first molar-maxillary segments consists of a compact substance and an insignificant amount of spongy substance. The bone beams are long, arranged vertically, running further into the palatine and zygomatic processes. The width of the periodontal gap in the gingival part reaches 0.35 mm, in the apical part – 0.55 mm.
7. The results of histological studies focusing on the periodontal ligament of the maxillary medial incisors reveal that the ratio of the specific area of loose connective tissue to similar indicators of dense connective tissue in the gingival part, middle third and apical part of the root is as follows: on the vestibular surface – 1/2,19, 1/5,68 and 1/5,52, respectively; on the oral surface – 1/3,39, 1/6,31 and 1/3,84, respectively; on the medial surface – 1/2,88, 1/4, 97 and 1/2,78, respectively; on the distal surface – 1/2,62, 1/3,75 and 1/3,15, respectively. The vestibular surface at the level of the root gingival part, and the oral surface at the level of the root apical part is the *periodontal ligament compression* area, while the oral surface at the level of the root gingival part and the vestibular surface at the level of the root apical part is the *periodontal ligament stretching* area.
8. The results of histological studies focusing on the periodontal ligament of the maxillary first molars show the following ratios of the specific area of loose connective tissue to similar indicators of dense connective tissue in the gingival part, middle third and apical part of the root: on the vestibular surface – 1/1,50, 1/1,99 and 1/2,43, respectively; on the oral surface – 1/2,34, 1/5,81 and 1/2,61, respectively; on the medial surface – 1/1,21, 1/2, 35 and 1/3,19, respectively; on the distal surface – 1/2,36, 1/3,29 and 1/3,46, respectively. At the level of the root gingival part, the medial and vestibular surfaces are the *periodontal ligament compression* areas, while the oral and distal surfaces are the *periodontal ligament stretching* area.
9. A quantitative assessment of the periodontal ligament structural elements of the medial incisors and the first molars in various parts of the maxilla root indicates that the specific area of loose connective tissue prevails in the *periodontal ligament compression* area, while the specific area of dense connective tissue is prevailing in the *periodontal ligament stretching* area during chewing load.
10. The results of a quantitative analysis focusing on the microvascular bed of the periodontal ligament of the medial incisors and the first molars in various parts of the maxilla root show that the area of blood vessels at the *compression* spots is significantly larger than the area of blood vessels to be observed at the *stretching* spots.

REFERENCES

1. ***Ash M. M.*** Wheeler's dental anatomy, physiology and occlusion. Philadelphia: WB Saunders; 2003.
2. ***Bassetti C.*** New concepts in maxillofacial bone surgery. – Berlin: Springer, 1976. – 194 p.
3. ***Clarke B***. Normal bone anatomy and physiology. *Clin J Am Soc Nephrol*. 2008 Nov;3 Suppl 3(Suppl 3):S131-9. DOI: 10.2215/CJN.04151206
4. Sobotta. Anatomy Textbook: English Edition with Latin Nomenclature / F. Paulsen, T. M. Böckers, J. Waschke. – Elsevier Health Sciences, 2018. - 840 p.
5. ***Dmitrienko S. V.*** Enhancement of research method for spatial location of temporomandibular elements and maxillary and mandibular medial incisors. *Archiv EuroMedica*. 2019. T. 9. № 1. P. 38-44. https://doi.org/10.35630/2199-885X/2019/9/1/38
6. ***Porfyriadis M.*** Major telerenthengogram indicators in people with various growth types of facial area. *Archiv EuroMedica*. 2018. Vol. 8; 1: 19-24. https://doi.org/10.35630/2199-885X/2018/8/1/19
7. ***Tefova K., Dmitrienko T., Kondratyeva T.*** Modern x-ray diagnostics potential in studying morphological features of the temporal bone mandibular fossa. *Archiv EuroMedica*. 2020. Vol. 10. № 1. P. 118-127. https://doi.org/10.35630/2199-885X/2020/10/36
8. ***Kochkonyan T. S., Al-Harazi G.*** Clinical types of hard palatal vault in people with various gnathic dental arches within physiologically optimal norm. *Archiv EuroMedica*. 2022. Vol. 12; 1: 91-98. – DOI 10.35630/2199-885X/2022/12/1.20
9. ***Dmitrienko T. D.*** Connection between clinical and radiological torque of medial incisor at physiological occlusion. *Archiv EuroMedica*. 2019. Vol. 9. № 1. P. 29-37. https://doi.org/10.35630/2199-885X/2019/9/1/29
10. ***Domenyuk D.*** Structural arrangement of the temporomandibular joint in view of the constitutional anatomy. *Archiv EuroMedica*. 2020. Vol. 10. № 1. P. 126-136. https://doi.org/10.35630/2199-885X/2020/10/37
11. ***Kochkonyan T. S., Shkarin V. V.*** Variant anatomy of transitional occlusion dental arch at optimal occlusal relationships. *Archiv EuroMedica*. 2022. Vol. 12; 2: 128-133. – DOI 10.35630/2199-885X

/2022/12/2.32

12. ***Ghamdan Al. H.*** A method for modeling artificial dentures in patients with adentia based on individual sizes of alveolar arches and constitution type. *Archiv EuroMedica*. 2021. Vol. 11; 1: 109–115. https://doi.org/10.35630/2199-885X/2021/11/1.25
13. ***Konnov V. V., Pichugina E.N., Frolkina K.M***. Jaw bones microarchitectonics and morphology in patients with diabetes mellitus. Archiv EuroMedica. 2022. Vol. 12; 6: 26. DOI 10.35630/2022/12/6.26
14. ***Ghamdan Al. H.*** Occlusal plane orientation in patients with dentofacial anomalies based on morphometric cranio-facial measurements. *Archiv EuroMedica*. 2021. Vol. 11; 1: 116–121. https://doi.org/10.35630/2199-885X/2021/11/1.26
15. ***Harutyunyan Yu.*** Undifferentiated connective tissue dysplasia as a key factor in pathogenesis of maxillofacial disorders in children and adolescents. *Archiv EuroMedica*. 2020. Vol. 10; 2: 83-94. https://dx.doi.org/10.35630/2199-885X/2020/10/2.24
16. ***Grinin V. M., Khalfin R. A.*** Specific features of transversal and vertical parameters in lower molars crowns at various dental types of arches. *Archiv EuroMedica*. 2019. Vol. 9; 2: 174-181. https://doi.org/10.35630/2199-885X/2019/9/2/174
17. ***Ivanyuta O., Al-Harasi G.*** Modification of the dental arch shape using graphic reproduction method and its clinical effectiveness in patients with occlusion anomalies // *Archiv EuroMedica*. 2020. Vol. 10; 4: 181-190. – DOI 10.35630/2199-885X/2020/10/4.42
18. ***Kochkonyan T. S., Al-Harazi G.*** Morphometric patterns of maxillary apical base variability in people with various dental arches at physiological occlusion. *Archiv EuroMedica*. 2021. Vol. 11; 4: 123-129. – DOI 10.35630/2199-885X/2021/11/4.29
19. ***Suetenkov D.E., Firsova I.V., Kubaev A***. A modified method for rapid palatal expansion anchored on mini-implants. *Archiv EuroMedica*. 2022. Vol. 12; 1: 84-90. DOI 10.35630/2199-885X/2022/12/1.19
20. ***Kochkonyan T.S., Shkarin V.V., Dmitrienko S.V***. Conceptual approach to diagnosing and treating dentoalveolar transversal divergent occlusion. *Archiv EuroMedica*. 2022. Vol. 12. No 3. P. 25. – DOI 10.35630/2199-885X/2022/12/3.25
21. ***Domenyuk D.A., Kochkonyan T.S.*** Implementation of neuromuscular dentistry principles in rehabilitation of patients with complete adentia. *Archiv EuroMedica.* 2022. Vol. 12; 2: 108-117. – DOI 10.35630/2199-885X/2022/12/2.29
22. ***Borodina V.V.*** Biometry of permanent occlusion dental arches – comparison algorithm for real and design indicators. *Archiv EuroMedica*. 2018. Vol. 8; 1. P. 25-26. DOI: 10.35630/2199-885X/2018/8/1/25
23. **23.** ***Kochkonyan T. S***. Periodontal tissue morphology in children with abnormal occlusion and connective tissue dysplasia syndrome // *Archiv EuroMedica*. 2022. Vol. 12; 5: 18. – DOI 10.35630/2199-885X/2022/12/5.18
24. **24**. ***Gilmiyarova F. N., Shkarin V. V***. Biochemical and immunohistochemical studies of matrix metalloproteinases in periodontal disease pathogenesis affecting children with connective tissue dysplasia syndrome // *Archiv EuroMedica*. – 2023. – Vol. 13, No. 1. DOI 10.35630/2023/13/1.219
25. ***Mazharov V. N.*** Peculiarities of the orientation of the occlusion plane in people with different types of the gnathic part of the face. *Medical News of North Caucasus*. 2021;16(1):42-46. DOI – https://doi.org/10.14300/mnnc.2021.16011 (In Russ.)
26. ***Sumkina O. B***. Histological and morphometric studies of bone tissue autografts from intraoral and extraoral donor zones // Archiv EuroMedica. 2023. Vol. 13; 2. – DOI 10.35630/2023/13/2.415
27. ***Domenyuk D. A.*** The potential of microcomputed tomography in studying the variant morphology of the dental canal-root system // *Archiv EuroMedica*. – 2021. – Vol. 11, No. 3. – P. 61-67. – DOI: 10.35630/2199-885X/2021/11/3/15
28. ***Lepilin A.V., Fomin I.V.*** Improving odontometric diagnostics at jaw stone model examination. *Archiv EuroMedica*. 2018. Vol. 8; 1: 34-35. https://doi.org/10.35630/2199-885X/2018/8/1/34
29. ***Porfyriadis M.P.*** Scanning electron microscopy and X-ray spectral microanalysis in dental tissue resistance // *Archiv EuroMedica*. 2019. Vol. 9; 1: 177-185. https://doi.org/10.35630/2199-885X/2019/9/1/177
30. ***Avanisyan V., Al-Harazi G.*** Morphology of facial skeleton in children with undifferentiated connective tissue dysplasia. Archiv EuroMedica. 2020. Vol. 10; 3: 130-141. https://dx.doi.org/10.35630/2199-885X/2020/10/3.32
31. ***Kochkonyan T.S., Shkarin V.V***. X-ray cephalometric features of nasal and gnathic sections in different facial skeleton growth types // *Archiv EuroMedica*. – 2022. – Vol. 12. – No 4. – P. 14. – DOI 10.35630/2199-885X/2022/12/4.14

32. ***Shkarin V. V., Dmitrienko S. V.*** Morphological features of dental arch shape and size within baby teeth bite period // *Archiv EuroMedica*. – 2022. – Vol. 12, No. 3. – P. 23. – DOI DOI: 10.35630/2199-885X/2022/12/3.23
33. ***Grinin V.M., Khalfin R.A.*** Specific features of grinder teeth rotation at physiological occlusion of various gnathic dental arches. *Archiv EuroMedica*. 2019. Vol. 9; 2: 168-173. https://doi.org/10.35630/2199-885X/2019/9/2/168
34. ***Korobkeev A. A.*** Anatomical and topographical features of temporomandibular joints in various types of mandibular arches. *Medical News of North Caucasus*. 2019;14(2):363-367. DOI – http://dx.doi.org/10.14300/mnnc.2019.14089 (In Russ.)
35. ***Kondratyeva T.*** Methodological approaches to dental arch morphology studying. *Archiv EuroMedica*. 2020. Vol. 10; 2: 95-100. https://dx.doi.org/10.35630/2199-885X/2020/10/2.25
36. ***Korobkeev A.A.*** Anatomical features of the interdependence of the basic parameters of the dental arches of the upper and lower jaws of man. *Medical news of North Caucasus*. 2018. – Vol. 13. – № 1-1. – P. 66-69. (In Russ., English abstract). DOI – https://doi.org/10.14300/mnnc.2018.13019
37. ***Dmitrienko S. V***. Specific features of x-ray anatomy and profilometry in people with different types of facial skeleton // *Archiv EuroMedica*. – 2022. – Vol. 12, No. 4. – P. 6. – DOI 10.35630/2199-885X/2022/12/4.6
38. ***Korobkeev A. A.*** Variability of odontometric indices in the aspect of sexual dimorphism. *Medical News of North Caucasus*. 2019;14(1.1):103-107. DOI – https://doi.org/10.14300/mnnc.2019.14062 (In Russ.)
39. ***Lepilin A.V.*** A biometric approach to diagnosis and management of morphological changes in the dental structure // *Archiv EuroMedica*. – 2020. – Vol. 10, No. 3. – P. 118-126. https://dx.doi.org/10.35630/2199-885X/2020/10/3.30
40. ***Rashmi G.S.*** Textbook of Dental Anatomy, Physiology and Occlusion. 1st ed. New Delhi: Jaypee Brothers Medical Publishers Ltd; 2014. DOI: 10.5005/jp/books/11841
41. ***Coskun O.*** Magnetic resonance imaging and safety aspects. Toxicol Ind Health. 2011 May;27(4):307-13. DOI: 10.1177/0748233710386413
42. ***Procop M.*** Spiral and Multislice Comuted Tomography of the Body/ M. Procop. – Berlin: Thieme, 2003. – 712 p.
43. ***Hansson B.*** Swedish national survey on MR safety compared with CT: a false sense of security? Eur Radiol. 2020 Apr;30(4):1918-1926. DOI: 10.1007/s00330-019-06465-5
44. ***Quarles L. D.*** Endocrine functions of bone in mineral metabolism regulation. J Clin Invest. 2008 Dec;118(12):3820-8. DOI: 10.1172/JCI36479
45. ***Zelensky V.A., Pushkin S.V.*** Peculiarities of phosphorine calcium exchange in the pathogenesis of dental caries in children with diabetes of the first type. *Entomology and Applied Science Letters.* 2018. Vol.5; 4. P. 49-64.
46. ***Tamamura Y.*** Bone and tooth in calcium and phosphate metabolism. *Clin Calcium*. 2012 Jan;22(1):11-7.
47. ***Courbebaisse M.*** Phosphocalcic metabolism: regulation and explorations. *Nephrol Ther*. 2011 Apr;7(2):118-38. DOI: 10.1016/j.nephro.2010.12.004
48. ***Davydov B.N., Budaychiev G.M-A.*** Changes of the morphological state of tissue of the paradontal complex in the dynamics of orthodontic transfer of teeth (experimental study). *Periodontology*, 2018; Vol. 23; 1-23(86): 69-78. DOI:10.25636/PMP.1.2018.1.15
49. ***Fukumoto S.*** Bone as an endocrine organ. *Trends Endocrinol Metab*. 2009 Jul;20(5):230-6. DOI: 10.1016/j.tem.2009.02.001
50. ***Fukumoto S***. The role of bone in phosphate metabolism. *Mol Cell Endocrinol*. 2009 Oct 30;310(1-2):63-70. DOI: 10.1016/j.mce.2008.08.031
51. ***Chen D.*** Bone morphogenetic proteins. *Growth Factors*. 2004 Dec;22(4):233-41. DOI: 10.1080/08977190412331279890
52. ***Christiansen P.*** The skeleton in primary hyperparathyroidism: a review focusing on bone remodeling, structure, mass, and fracture. APMIS Suppl. 2001;(102):1-52.
53. ***Davydov B.N***. Modern possibilities of clinical-laboratory and x-ray research in pre-clinical diagnostics and prediction of the risk of development of periodontal in children with sugar diabetes of the first type. Part I. *Periodontology*, 2018; Vol. 23; 3-23(88): 4-11. DOI:10.25636/PMP.1.2018.3.1
54. ***Steiniche T.*** Bone histomorphometry in the pathophysiological evaluation of primary and secondary osteoporosis and various treatment modalities. APMIS Suppl. 1995;51:1-44**.**
55. ***Davydov B.N***. Improving diagnostics of periodontal diseases in children with connective tissue dysplasia based on X-ray morphometric and densitometric data. *Periodontology*.2020;25(4):266-275.

(in Russ.) https://doi.org/10.33925/1683-3759-2020-25-4-266-275

56. ***Seeman E***. Reduced bone formation and increased bone resorption: rational targets for the treatment of osteoporosis. Osteoporos Int. 2003;14 Suppl 3:S2-8. DOI: 10.1007/s00198-002-1340-9
57. ***Samedov F.*** Matrix metalloproteinases and their tissue inhibitors in the pathogenesis of periodontal diseases in type 1 diabetes mellitus // *Archiv EuroMedica*. 2019. Vol. 9;3. P. 81-90. https://doi.org/10.35630/2199-885X/2019/9/3.25
58. ***Cefalu C. A***. Is bone mineral density predictive of fracture risk reduction? *Curr Med Res Opin*. 2004 Mar;20(3):341-9. DOI: 10.1185/030079903125003062
59. ***Boron W. F***. Medical physiology: a cellular and molecular approach / W.F. Boron, E.L. Boulpaep. – 2nd Rev. ed. – Saunders, 2008. – 1352 p.
60. ***Kim J. K***. Anatomical variability of the maxillary artery: findings from 100 Asian cadaveric dissections. *Arch Otolaryngol Head Neck Surg*. 2010 Aug;136(8):813-8. DOI: 10.1001/archoto.2010.121
61. ***Hur M. S.*** Clinical implications of the topography and distribution of the posterior superior alveolar artery. *J Craniofac Surg*. 2009 Mar;20(2):551-4. DOI: 10.1097/SCS.0b013e31819ba1c1
62. ***Rosano G***. Maxillary sinus vascularization: a cadaveric study. *J Craniofac Surg*. 2009 May;20(3):940-3. DOI: 10.1097/SCS.0b013e3181a2d77f

back